Publication Title: Cyber-Attacks in a Looped Energy-Water Nexus: An Inoculated Sub-Observer Based Approach
Authors: Haris M. Khalid, S. M. Muyeen, and Jimmy C.-H. Peng

DOI: 10.1109/JSYST.2019.2941759

Cyber-Attacks in a Looped Energy-Water Nexus: An Inoculated Sub-Observer Based Approach

Haris M. Khalid, *Member, IEEE,*, S. M. Muyeen, *Senior Member, IEEE*, and Jimmy C.-H. Peng, *Member, IEEE*

***Abstract*—The deployment of advanced sensors has strengthened the monitoring capability of power plants. In the context of cogeneration process, the plant cooling is performed by the cooling towers using condensation process on exhaust steam. However, the computer networks and industrial control systems built on this sensor-based digital layer may become vulnerable to cyber-attacks. This may eventually raise a concern on the performance and security of these energy utilities. To resolve this issue, an inoculated sub-observer based fusion filter (SOFF) is proposed. It improves the resilience against malicious attacks in combined cycle power plants with desalination units, which are usually functioning in a closed-loop environment and infected with injected-attacks. A time-delay based state representation is considered for the system. To access latency in a closed-loop environment, a subsystem-based set of sub-observers are introduced. Information from each sensor is then gathered using the interacting multiple model (IMM)-based fusion process. The stability of the system has been proved and kept in-check at two different implementation levels of the procedure using functional equivalence and Lyapunov stability criteria respectively. Performance evaluation is then conducted on a water level system. Results show the proposed scheme accurately extracted the system parameters from the contaminated measurements in the presence of multiple system disturbances and cyber intervention.**

***Index Terms*—Closed-loop systems, cool water basin, cooling towers, cyber-attacks, cyber-physical systems, data fusion, energy-water nexus, intrusion detection, liquid-level control, power and water desalination plant, quadruple tank system, security, sub-observer, time-delay, water utility.**

I. Introduction

THE scarcity of potable water lead to the concept of hybrid power and water desalination plants in Middle-East and North Africa (MENA) region [1]. Large volumes of brackish water are accessed from the sea, and further utilized by the combined-cycle gas turbine units for: 1) electricity generation, and 2) potable water processes using desalination. In combined-cycle gas turbine, the water-based plant cooling system represent almost all of the power plant cooling requirements [2]. With increased industrial development and economic growth, this energy-water nexus operation has expanded by relying on advance sensor-based remote monitoring systems. For example, ABB has provided solutions like next level control center, OPTIMAX® and Symphony-Plus® to increase situational awareness of power plants [3–5]. These solutions have designed support functions to the industries, with particular focus on factors such as: 1) improve availability of plant components, 2) optimal operational, and 3) maintenance cost. However, equal weightage should be given to the fact that the water-energy systems have been connected to the internet for an ade-

H. M. Khalid is with the Department of Electrical and Electronics Engineering, Higher Colleges of Technology (HCT), Sharjah 7947, UAE, (e-mail: *harism.khalid@yahoo.com*, webpage: *www.harismkhalid.com*)

S. M. Muyeen is with the School of Electrical Engineering Computing and Mathematical Sciences, Curtin University, Australia, (email: *s.m.muyeen@ieee.org*)

J. C.-H. Peng is with the Department of Electrical and Computer Engineering, National University of Singapore, Singapore, (e-mail: *jpeng@nus.edu.sg*, webpage: *www.penglaboratory.com*)

Acronyms and Abbreviations of Mathematical Formulations

IMM	interacting multiple model
FD	fault diagnosis
HPC	high performance computing
HRSG	heat recovery steam generator
MENA	Middle-East and North Africa
MIMO	multi-input multi-output
MSE	mean-square error
SOFF	sub-observer based fusion filter
UKF	Unscented Kalman Filter
$\mathbf{E}$	expectation operator
N	number of measurements
$\hat{h}$	rate of change of water-level
t	time-instant
Q	water flow storage demand
a	tank cross-sectional area
a_{pipe}	pipe cross-sectional area
Q_c	water flow consumption demand
$\frac{\Delta h}{\Delta t}$	velocity of water feed-flow
τ_s	sampling-time
$(\tau_{\mathcal{F}}, \tau_{\psi}, \tau_C, \tau_d)$	set of time-delay
$(h^{\mathcal{U}}, h^{\mathcal{V}}, ... \ h^{\mathcal{Z}})$	set of water-tanks
$(q^{\mathcal{U}}, q^{\mathcal{V}}, ... \ q^{\mathcal{Z}})$	set of water-pumps
h^H	system's water level state
n	state-vector size
$\mathbf{R}$	subspace
$\mathcal{F}^H$	modal matrix of liquid-level height
V^Q	voltage supplied to the pump
Ψ_j^Q	transition matrix for pump voltage
G	noise transition
w	random process noise
y	simultaneous observations
C	observation
v	observation noise
$d(a_l)$	attack-vector function
$\bar{o}$	size of attack vector
$\mathcal{C}$	size of set $\mathcal{A}$
h_1	state of subsystem 1
h_2	state of subsystem 2
o	outlet cross-sectional area
g	acceleration due to gravity
$\bar{w}, \bar{v}$	resultant noises
K_p	pump-flow constant
$\aleph$	process noise correlation factor
δ	Kronecker delta function
K	filter gain
$\tilde{h}$	difference between state and its estimate
I	identity matrix
P	filter error covariance
ω	computing weight
$\mathcal{Z}$	possible height models for water-level
A_1, A_2, A_3, A_4	matrix variables
$\mathcal{L}_0$	Lyapunov function
R	covariance error
ξ	variation parameter
e_{res}	residual
Γ_{stat}	test statistic
λ	Likelihood ratio
η_{th}	threshold value

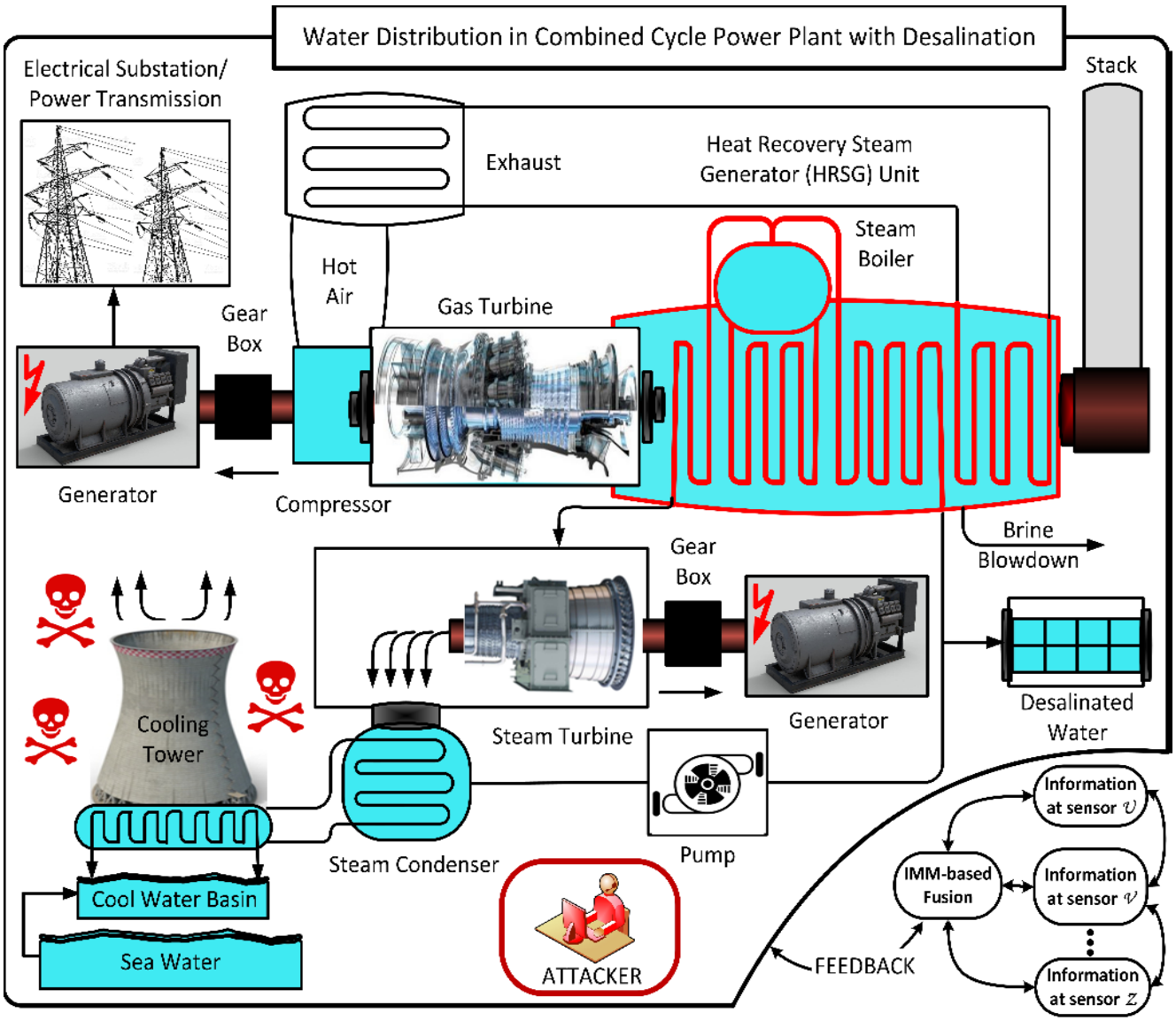

Fig. 1. Proposed SOFF scheme to estimate and detect cyber-attacks in water utility sector

quate implementation of these solutions. Thus, while providing provision to access more plant operations and remote monitoring, it also opened a window for hackers. This window could provide access to the critical infrastructure, followed by the breach of security and thus an emerging public risk. Such a risk is recently recorded by ABB, where two vulnerabilities[1] 1) Meltdown (CVE-2017-5754), and 2) Spectre (CVE2017-5753, CVE-2017-5715) have affected the processors [6]. Such risks could eventually leave thousands of kilometers of pipes, pumps, valves, and water distribution systems inherently vulnerable to cyber-attack [7, 8], and raising concerns over the robustness of energy-water nexus. The focus of this paper is towards cyber-security of cool water basin in plant cooling and its distribution towards: 1) electricity generation, and 2) potable water processes using desalination.

The maintenance of hydraulic plants can be made effective by integrating a fault diagnosis (FD) scheme into the system [9–14]. The FD schemes are incorporated as an integral part of the system with a focus to look into the occurrence of breakdown and system faults, such as component failure faults, fluid contamination, pipe leakage fault, material wear etc. [15–17]. With an hindsight, these FD functions could also help the cause of monitoring cyber-attacks in one way or another, since system failure is an obvious by-product of an attack. However, the situation around this concern could become more challenging and worse if some of these failures are the deliberate actions of an hacker. For instance: 1) a deliberate system contamination, 2) a wilful influence on physical processes of the system through closed-loop feedback actuation, and 3) a pre-determined material wear to divert the focus of the control center from major plant operations. Despite several methods proposed for cyber-attacks in general [18–20] and for hydraulic systems [21–24], none explored the problem of handling dynamics of an energy-water nexus, and that too in a closed-loop environment. Thus, the motivation of this paper is to improve the resilience of the

[1] Note there are no vulnerabilities specific to ABB. These situations are related to microprocessors in general which could effect the control devices of the plants.

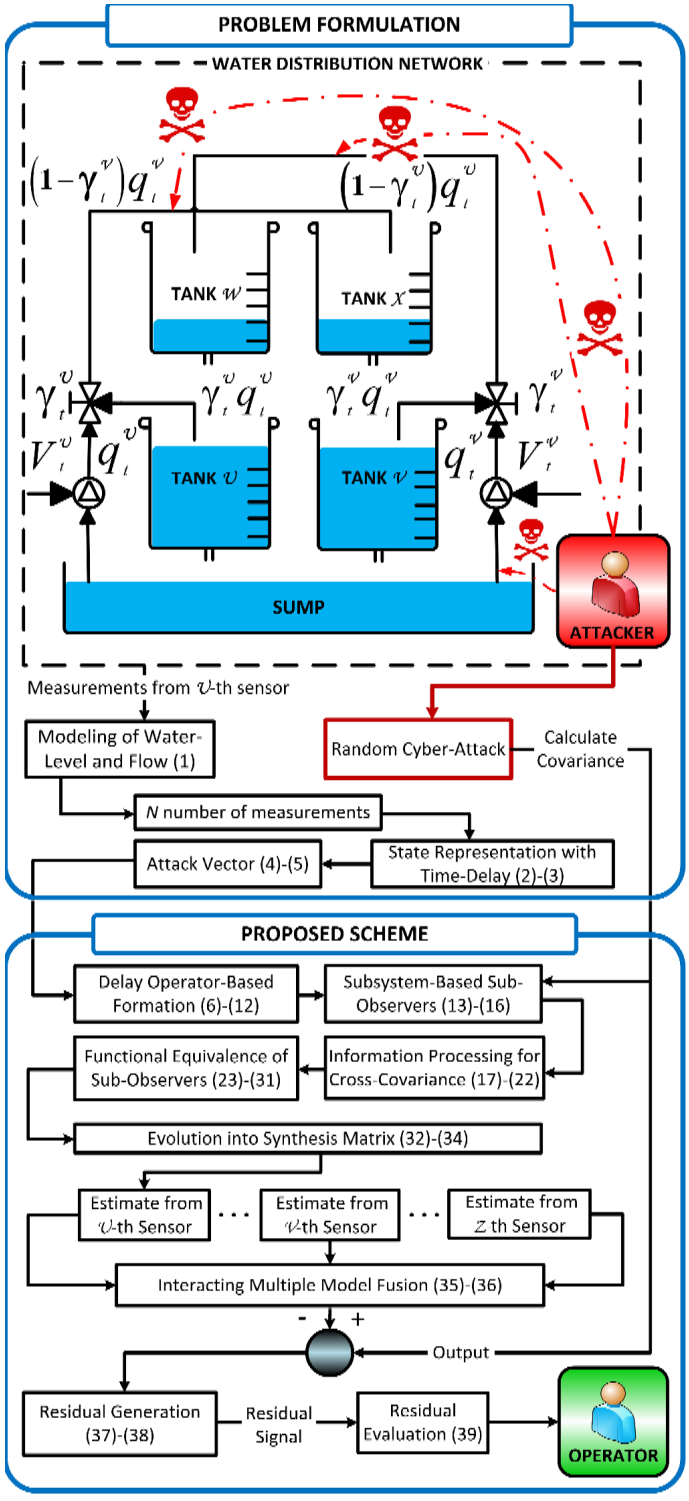

Fig. 2. Formulation framework of the proposed scheme

system while making it inoculated against cyber-attacks in a closed-loop environment.

Closed-loop systems at industrial-level have always been utilized to tackle the situational processes for those physical quantities and parameters, which may vary constantly and require a measure-decide-actuate sequence from the control loop. In energy-water systems, these physical quantities could be a set-point temperature of different processes, speed of the pump, water-level in the cooling tower etc. Since, feedbacks cannot be removed due to various reasons such as: 1) generation of data, 2) complexity of the process, and 3) production quality reasons, closed-loop identification has received considerable attention in system identification literature [25–27]. From the perspective of cyber-physical systems, the closed-loop brings additional challenges of time-delay and undetectable attacks. To the best of author's knowledge, such a situation has not been investigated in the context of energy-water systems.

Therefore, this paper proposed a signal processing solution to enhance the immunity of digital measurements against cyber-attacks and system breakdowns. A sub-observer based fusion filter (SOFF) is derived to augment the hinderance of the hydraulic system against the contaminated measurements. The aim is to maintain the accuracy of the digital measurements extracted as well as detecting and isolating the sensors compromised by the cyber-attacks. To understand the integration of cyber-attacks into the energy-water application, an overview of the proposed SOFF approach is illustrated in Fig. 1. A detailed figure of water distribution in combined cycle gas turbine-based power generation with desalination unit is represented. The considered scenario assumed that the attacker has accessed the cool water basin in plant cooling system. This could further make the water network vulnerable, especially the connected processors such as condenser, steam turbine, heat recovery steam generator (HRSG) unit, and the desalinated water. This could also affect the components that make system adequate for water distribution such as the water tank, pipes, their manifolds, pumps, motors, and timers. To maximize the damage while remaining undetected, the injected attacks may imitate regular variations, and can eventually drain the cooled water or push the limits of actuators. The proposed scheme can tackle this situation by estimating the parameters extracted from all the installed sensors. The estimated parameters are collected efficiently using IMM-based fusion, which considers the model probabilities and mixed estimate to ensure adequate collection. Note each installed sensor is employed with a sub-system based set of sub-observer to extract the dynamic parameters, and further provide their estimate. Also, each sensor is able to communicate with its neighboring sensors through time-based communication sequence. A number of steps of procedure are adopted here to handle a closed-loop working system. The proposed scheme provides a novel and convenient way to enhance the immunity of the system by making the parametric estimations at states, which are dominated by non-linearity and system perturbations.

Notations: In this paper, **E** is the expectation operator. When any of the variables become a function of time, the time index t appears as a subscript (e.g. h_t, C_t, y_t). When any of these variables are collected from sensors ($\mathcal{U}$, $\mathcal{V}$, ... $\mathcal{Z}$) installed at tanks or pumps, it will appear as a part of superscript (e.g. $h_t^{\mathcal{U}}$, $h_t^{\mathcal{V}}$, $q_t^{\mathcal{U}}$, $q_t^{\mathcal{V}}$). When any of these variables are collected from a subsystem 1 or 2, it will appear as a part of subscript (e.g. $h_{1,t}$, $h_{2,t}$, $C_{1,t}$, $C_{2,t}$, $y_{1,t}$, $y_{2,t}$).

The paper is organized as follows: The problem formulation is presented in Section II. The proposed scheme is formulated

in Section III, followed by its evaluation in Section IV. Finally conclusions are drawn in Section V.

II. Problem Formulation: Water Level System Under Attack

The problem formulation of the water level system under attack is derived in this section. An overview of the framework is illustrated in Fig. 2. It is assumed that the cool water basin is a water level system which is supplying water for condensate and steam turbine to tank $\mathcal{U}$, and for heat recovery steam generator to tank $\mathcal{V}$ respectively. The process is portrayed using a quadruple tank system. Fig. 2 summarizes the steps involved in problem formulation as follows: N number of measurements are collected from each sensor installed in the water-level system. In (1), these measurements are modeled for water-level and flow. This results in development of time-delay based dynamic model and an observation model of the system in (2) and (3). An attack vector is modeled in (4) and (5).

The quadruple tank system is one of the most widely used laboratory system for liquid-level control [28, 29]. It represents various industrial applications while providing features of multi-input multi-output (MIMO) and non-linear dynamics. Note the tank configuration may be classified into various types [30, 31]. This is based on the system configuration and the interaction required between the tanks.

A. Modeling of Water-Level and Flow

Consider a liquid-level control unit having multiple water tanks and actuators. In this unit, each tank is monitored by a level sensor and each actuator (pump) is equipped with a flow sensor. These sensors monitor the dynamics of water-level as follows:

$$\hat{h}_t = \frac{Q_t}{a} = \frac{a_{\text{pipe}}}{a}\left(\frac{\Delta h}{\Delta t}\right) - \frac{Q_{c,t}}{a} \tag{1}$$

where $\hat{h}_t$ is the rate of change of water-level at time-instant t, Q_t is the water flow storage demand, a is the cross-sectional area of the tank, and a_{pipe} is the pipe cross-sectional area. $Q_{c,t}$ is the water flow consumption demand, $\frac{\Delta h}{\Delta t}$ represents the velocity of feed-flow of water. The physical system exhibits a highly non-linear behavior. The flow rate saturates at 4.5 liters per second. The dead-band effect in the actuator exhibits itself as a delay in the output response, thereby making steady-state non-zero. All sensors are operating at the same sampling rate, τ_s of 50 milliseconds. Note the plant unit is a closed-loop system under sensor-attack. Therefore, it possesses properties of time-delay τ at: 1) input, 2) output, 3) plant states, and in 4) undetectable sensor attack.

B. State Representation of the Plant with Time-Delay

While system is under sensor attack, it has been initially assumed that there is no loss of generality between the sensors. The plant can be represented by a general discrete-time dynamic model with time-delay as:

$$h^H_{t+1} = \sum_{i=0}^{\tau_{\mathcal{F}}} \mathcal{F}^H_i h^H_{t-i} + \sum_{j=0}^{\tau_\Psi} \Psi^Q_j V^Q_{t-j} + G_t w_t \tag{2}$$

$$y_t = \sum_{k=0}^{\tau_C} C^H_k \mathcal{F}^H_{t-k} h^H_t + \sum_{l=0}^{\tau_d} d(a_l) V^Q_{t-j} + v_t \tag{3}$$

where $h^H_t \in \mathbf{R}^{n\times 1}$ denote the system's state of water level at time-instant t with $H = [h^{\mathcal{U}}_t, h^{\mathcal{V}}_t, ... h^{\mathcal{Z}}_t]$ for $\mathcal{Z}$ number of water tanks in the plant. Superscript n is the size of state vector in subspace $\mathbf{R}$. $\mathcal{F}^H_i \in \mathbf{R}^{n\times n}$ is a modal matrix of state response of height of liquid level, such that $i = 0, ..., \tau_{\mathcal{F}}$. $V^{\mathcal{Q}}_t \in \mathbf{R}^{n\times 1}$ is the voltage supplied to the pump for an adequate water flow with $Q = q^{\mathcal{U}}_t, q^{\mathcal{V}}_t, ..., q^{\mathcal{Z}}_t$ for $\mathcal{Z}$ number of pumps in the plant. $\Psi^Q_j \in \mathbf{R}^{n\times n}$ is the transition matrix for pump voltage, such that $j = 0, ..., \tau_j$. $G_t \in \mathbf{R}^{n\times n}$ is the noise transition, which can be defined as a probability vector, whose elements are non-negative real numbers and sum to 1. $w_t \in \mathbf{R}^{n\times 1}$ is the random process noise. In the observation model (3), $y_t \in \mathbf{R}^{m\times 1}$ is the number of simultaneous observations obtained from m sensor of set $S = \{1, 2, ...m\}$ at time-instant t. The observations were $C^H_k \in \mathbf{R}^{m\times m}$, such that $k = 0, ..., \tau_k$. $v_t \in \mathbf{R}^{m\times 1}$ is the observation noise. $d(a_l) \in \mathbf{R}^{\bar{o}\times 1}$ is the attack-vector function.

C. Attack Vector

The attack vector is represented in the observation model (3) such that $d(a_l) \in \mathbf{R}^{\bar{o}\times 1}$. Here $d(a_l)$ denotes the function of an attack vector and is unknown to the system such that $l = 0, ..., \tau_d$, where superscript $\bar{o}$ belongs to the set $\mathcal{A} \subseteq \{1, 2, ...\bar{o}\}$. It contains level and flow sensors installed in the plant which are under attack. This shows the attack vector for any $\mathcal{U}$-th and $\mathcal{V}$-th sensor as $d(a^{\mathcal{UV}}_l) = 0$, where $\mathcal{U} \in \mathcal{A}^{\mathcal{C}}$, and $\mathcal{V} \geq 0$. Superscript $\mathcal{C}$ represents the size of the set $\mathcal{A}$, such that $\mathcal{A}^{\mathcal{C}} = \frac{S}{\mathcal{A}}$. This also employs that $\sup(a^{\mathcal{V}}_l) \subseteq \mathcal{A}$ for all $\mathcal{V} \geq 0$. The function $d(a_l)$ itself represent the stochastic nonlinearity, such that:

$$\mathbf{E}[d(a_l)|h^H_{t-i}] = 0 \tag{4}$$

Also,

$$\mathbf{E}[d(a^{\mathcal{U}}_l)d'(a^{\mathcal{V}}_l)] = 0, \mathcal{U} \neq \mathcal{V}, \tag{5}$$

where superscript '$'$' represents the transpose operator.

Once the attack vector is modeled on the measurements, which are extracted from the affected part, the proposed scheme is formulated.

III. Proposed Scheme

An overview of the proposed scheme can be seen in the framework of Fig. 2. A delay operator-based equivalent formation of system is made in (6)-(12). This is a time-delay free formation, which is introduced to reverse generality and presence of symmetry in the system. To achieve precision, the formation model is formulated towards subsystem-based set of sub-observers in (13)-(16). This step is further processed to collect information on cross-covariance at (17)-(22), and functional equivalence at (23)-(31). The sub-observers are synthesized into the main system at (32)-(34). This now calls for the fusion of information at (35)-(36), residual generation (37)-(38), and residual evaluation (39) respectively.

To preserve generality and presence of symmetry, a delay operator is introduced for equivalent formation of systems which are free of time-delay.

A. Delay Operator-based Equivalent Formation

A delay operator ∇ is defined here for the plant state h_t in the form of polynomial matrices, such that $\nabla_{\tau_\mathcal{F}} h_t = h(t-\tau_\mathcal{F})$, with $\tau_\mathcal{F} \in \mathbf{N}$. Implying this delay operator in (2) gives a variable $\breve{h}_t$ as:

$$\breve{h}_t = T[\nabla] h_t \tag{6}$$

where $T[\nabla] \in \mathbf{R}[\nabla]^{n\times n}$. This property defines the following lemma for (2)-(3).

Lemma III.1: The original liquid level control plant (2)-(3) implies the delay operator as in (6), if and only if there exist $T_i \in \mathbf{R}^{n\times n}$ for $i = 0, 1, ..., \tau_m$ with $\tau_m = \sup(\tau_\mathcal{F}, \tau_\psi, \tau_C, \tau_d)$. For supremum of $\tau_\mathcal{F}$,

$$\sum_{i=0}^{k} T_i \mathcal{F}_{k-i} = \bar{\mathcal{F}}_k T_k,\ k = 0, 1, ... \tau_m + \tau_\mathcal{F} \tag{7}$$

where $\bar{\mathcal{F}}_t = \breve{\mathcal{F}}_t$ and $\bar{\mathcal{F}}_k = 0, \forall\ k > 0$. For supremum of τ_ψ,

$$\sum_{i=0}^{k} T_i \Psi_{k-i} = \bar{\Psi}_k T_k,\ k = 0, 1, ...\tau_m + \tau_\Psi \tag{8}$$

where $\bar{\Psi}_t = \breve{\Psi}_t$ and $\bar{\Psi}_k = 0, \forall\ k > 0$. $\sup(\tau_C)$ gives:

$$\sum_{i=0}^{k} T_i C_{k-i} = \bar{C}_k T_k,\ k = 0, 1, ... \tau_m + \tau_C \tag{9}$$

where $\bar{C}_t = \breve{C}_t$ and $\bar{C}_k = 0, \forall\ k > 0$. $\sup(\tau_d)$ gives:

$$\sum_{i=0}^{k} T_i d(a_{k-i}) = \bar{d}(a_k) T_k,\ k = 0, 1, ... \tau_m + \tau_{d(a)} \tag{10}$$

where $\bar{d}(a_t) = \breve{d}(a_t)$ and $\bar{d}(a_k) = 0, \forall\ k > 0$.

The determinant of the delay operator can be defined as: $\det(\sum_{i=0}^{\tau_m} T_i \nabla^i) \in \mathbf{R}$. This gives equivalent formation of (2)-(3) as:

$$\breve{h}^H_{t+1} = \breve{\mathcal{F}}^H_t \breve{h}^H_t + \breve{\Psi}^Q_t V^Q_t + G_t w_t \tag{11}$$

$$y_t = \breve{C}_t \breve{\mathcal{F}}^H_t h^H_t + \breve{d}(a_t) V^Q_t + v_t \tag{12}$$

Note the above formation exists if and only if the conditions in *Lemma II.1* satisfy.

Once the delay-based equivalent formation is made, the plant model is further analyzed. To estimate $\breve{h}^H_t$ in (11) and (12) from y_t may be a difficult problem. This is both due to the dynamic system and a possible nonlinear function-based cyber attack. This will eventually result in 1) a compromise to access the latency in liquid-level and flow in the presence of cyber-attack, 2) difficulty in tackling the computational cost to estimate the plant states and their covariates. To overcome these challenges, a subsystem-based set of sub-observer approach has been proposed.

B. Subsystem-Based Set of Sub-Observers

A quadruple tank system was used to formulate and derive the subsystem-based set of sub-observers [32]. Consider a quadruple tank system, which consists of four water tanks driven by two pumps as shown in Fig. 2. The aim is to control the water levels $h^\mathcal{U}_t$ and $h^\mathcal{V}_t$ of the lower tanks $\mathcal{U}$ and $\mathcal{V}$ respectively. The inputs of this tank based liquid-level control problem are the voltages $V^\mathcal{U}_t$ and $V^\mathcal{V}_t$ of pumps $\mathcal{U}$ and $\mathcal{V}$ respectively. The outputs are the corresponding water levels in the tanks $h^\mathcal{U}_t$ and $h^\mathcal{V}_t$. All the dynamics are monitored by installed sensors. The system can actually be represented by the dynamic model of (11)-(12), such that $H = \{h^\mathcal{U}_t,\ h^\mathcal{V}_t,\ h^\mathcal{W}_t,\ h^\mathcal{X}_t\}$. The system can then be further transformed into the following two subsystem-based set of sub-observers. This is achieved by introducing transformation of (11), such that $\breve{h}^H_t = R[h^{'}_{1,t}\ \ h^{'}_{2,t}]'$ with $h_{1,t} \in \mathbf{R}^{n_1\times 1}$ and $h_{2,t} \in \mathbf{R}^{n_2\times 1}$ as:

$$h^H_{1,t+1} = \mathcal{F}_{0,t} h^{H,\frac{1}{2}}_{1,t} + \Psi_{0,t} V^\mathcal{U}_t + \Psi_{1,t} V^\mathcal{U}_t + \Psi_{2,t} V^\mathcal{V}_t + G_t w_t \tag{13}$$

$$h^H_{2,t+1} = \bar{\mathcal{F}}_{0,t} h^{H,\frac{1}{2}}_{2,t} + \bar{\Psi}_{0,t} V^\mathcal{U}_t + \bar{\Psi}_{1,t} V^\mathcal{U}_t + \bar{\Psi}_{2,t} V^\mathcal{V}_t + G_t \bar{w}_t \tag{14}$$

$$y_t = C_t \mathcal{F}_t h_t + d(a_t) + \bar{v}_t \tag{15}$$

where $h_{1,t}$ and $h_{2,t}$ are states of subsystem 1 and 2 representing the full dynamics of the quadruple tank system. A bar '-' is used to represent transition matrices of subsystem 2. In (13) $\mathcal{F}_{0,t} = -\frac{o\sqrt{2g}}{a}$, where o is the cross-sectional area of an outlet, g is the acceleration due to gravity, and a is the cross-sectional area of the tanks. $\Psi_{0,t} = \frac{\gamma^\mathcal{U}_t K_p}{a}$ where $\gamma^\mathcal{U}_t$ is the ratio of liquid flow generated from the voltage supply $V^\mathcal{U}_t$ for pump $\mathcal{U}$, and K_p is the pump-flow constant. $\Psi_{1,t} = \frac{K_p}{a}$, $\Psi_{2,t} = -\frac{\gamma^\mathcal{V}_t K_p}{a}$, where $\gamma^\mathcal{V}_t$ is the ratio of liquid flow generated from the voltage supply $V^\mathcal{V}_t$ for pump $\mathcal{V}$. In (14) $\bar{\mathcal{F}}_0 = -\frac{o\sqrt{2g}}{a}$, $\bar{\Psi}_{0,t} = \frac{K_p}{o\sqrt{2g}}$, $\bar{\Psi}_{1,t} = -\frac{\gamma^\mathcal{U}_t K_p}{o\sqrt{2g}}$, and $\bar{\Psi}_{2,t} = -\frac{\gamma^\mathcal{V}_t K_p V^\mathcal{V}_t}{o\sqrt{2g}}$. Referring to (13)-(15), the resultant noises $\bar{w}_t$ and $\bar{v}_t$ will have a diagonalizable expected value as:

$$\mathbf{E}[\begin{bmatrix} \bar{w}_t \\ \bar{v}^{1'}_t \end{bmatrix}], [\bar{w}^{'}_t\ \bar{v}^{2'}_t] = \aleph^{1,2}_t \delta^{1,2}_t \tag{16}$$

where $\aleph^{1,2}_t$ is the process noise correlation factor between subsystem 1 and 2, $\delta^{1,2}_t$ is the Kronecker delta function used for shifting the integer variable after the presence or absence of noise. Note the control input for the whole system are the voltages generated from pump $\mathcal{U}$ and $\mathcal{V}$. Pump $\mathcal{U}$ provided interaction to tank $\mathcal{U}$ and tank $\mathcal{X}$ as $\gamma^\mathcal{U}_t K_p V^\mathcal{U}_t$ and $(1-\gamma^\mathcal{U}_t) K_p V^\mathcal{U}_t$ respectively. Similarly, pump $\mathcal{V}$ provides interaction to tank $\mathcal{V}$ and tank $\mathcal{W}$ as $\gamma^\mathcal{V}_t K_p V^\mathcal{V}_t$ and $(1-\gamma^\mathcal{V}_t) K_p V^\mathcal{V}_t$ respectively. This fulfills the developed notion of sub-observers since the liquid level and flow control is estimated by formulating pump flow towards the liquid tanks. Note in this paper, monitoring quadruple tank system to enhance the immunity of digital measurements against cyber-attacks and closed-loop system breakdown is used as an application. The proposed scheme can be utilized by any other application as well.

Once the subsystems-based set of sub-observers are constructed to provide the accessibility and enhanced observability towards any variations of cyber-induced attacks, a tool is required which can cross-verify the results extracted from the subsystems-based sub-observer model to avoid any false-alarms and unusual shutdown of the system. A calculation for the quantitative assessment of the similarity of the measured and estimated signal was opted. This calculation was made by cross-covariance analysis to find features of possible deviations, time shifts or time-lag caused by the induced cyber-attack.

C. Information Processing for Cross-Covariance

1) Prediction and Filtering Error Equations: Suppose the recursive equation of state $h^H_{1,t}$ is computed as:

$$h^H_{1,t+1|t+1}= \tilde{\mathcal{F}}_{0,t}(I_{n_1}-K_{1,t}C_t)\tilde{h}^H_{1,t|t-1}+\Psi_{0,t}(I_{n_1}-K_{1,t}C_t) \tilde{V}^{\mathcal{U}}_{t|t-1}+(\Psi_{1,t}+\Psi_{2,t})(I_{n_1}-K_{1,t}C_t)\tilde{V}^{\mathcal{V}}_{t|t-1} + G_t w_t-(\tilde{\mathcal{F}}_{0,t}K_{1,t}+J_t)\bar{v}_t \quad (17)$$

where $\tilde{h}^H_{1,t|t-1}$ is the difference between $h^H_{1,t}$ and $\hat{h}^H_{1,t|t-1}$, $\tilde{\mathcal{F}}_{0,t} = \mathcal{F}_{0,t} - J_t\bar{C}_t$, $J_t = G_t\aleph^{-1}_{\bar{v}_t}$, $\mathcal{F}_{0,t} = \tilde{F}_t - (I_{n_1} - K_{1,t}C_t) - G_t\aleph^{-1}_{\epsilon,t}\bar{C}_t$. I_{n_1} is an $n_1 \times n_1$ identity matrix. $K_{1,t}$ is the filtering gain. The corresponding updated *a-posteriori* equation of state $h^H_{1,t}$ will be:

$$\tilde{h}^H_{1,t|t} = (I_{n_1}-K_{1,t}\tilde{C}_t)\Big[\tilde{h}^H_{1,t|t-1}+(\tilde{V}^{\mathcal{U}}_{t|t-1}+\tilde{V}^{\mathcal{V}}_{t|t-1}) - \frac{(K_t\tilde{v}_t)}{(I_{n_1}-K_{1,t}\tilde{C}_t)}\Big] \quad (18)$$

where $\tilde{h}^H_{1,t|t}$ is the difference between $h^H_{1,t}$ and $\hat{h}^H_{1,t|t}$. Once the updated and predicted error equations of liquid-level state $h^H_{1,t}$ of subsystem 1 is achieved, the state $h^H_{2,t}$ of the subsystem 2 can be expressed as:

$$\tilde{h}^H_{2,t|t} = [\bar{\mathcal{F}}_{0,t}(I_{n_1} - K_{2,t}\bar{C}_t) - G_t\aleph^{-1}_{\varepsilon,t}\bar{C}_t]\tilde{h}^H_{1,t|t-1} + [(\bar{\Psi}_{0,t}+\bar{\Psi}_{1,t})(I_{n_1} - K_{2,t}\bar{C}_t) - G_t\aleph^{-1}_{\epsilon,t}\bar{C}_t]V^{\mathcal{U}}_t + [\bar{\Psi}_{2,t}(I_{n_1} - K_{2,t}\bar{C}_t) - G_t\aleph^{-1}_{\epsilon,t}\bar{C}_t]V^{\mathcal{V}}_t + [G_t, (-\bar{F}_{0,t}, -\bar{\Psi}_{0,t}, \bar{\Psi}_{1,t}, \bar{\Psi}_{2,t})K_{2,t} - G_t\aleph^{-1}_{\epsilon,t}][w^{'}_t, v^{'}_t]' \quad (19)$$

2) Cross-Covariance of Subsystem 1 $h^H_{1,t}$: Cross-covariance equation of the prediction and filtering errors of state $h^H_{1,t}$ between subsystem 1 and 2 can be computed as:

$$\begin{aligned} &P^{1,2}_{1,t+1|t+1}= \\ &\tilde{\mathcal{F}}_{0,t}[I_{n_1}-K_{1,t}\bar{C}_{1,t}]P^{1,2}_{1,t|t-1}[I_{n_1}-K_{1,t}\bar{C}_{2,t}]^{'} +\Psi_{0,t}[I_{n_1} \\ &- K_{1,t}\bar{C}_{1,t}]P^{1,2}_{1,t|t-1}[I_{n_1}-K_{1,t}\bar{C}_{2,t}]^{'}+(\Psi_{1,t}+\Psi_{2,t})[I_{n_1} \\ &- K_{1,t}\bar{C}_{1,t}]^{'}P^{1,2}_{1,t|t-1}[I_{n_1}-K_{1,t}\bar{C}_{2,t}]^{'}+[G_t-\bar{\mathcal{F}}_{0,1,t}K_{1,t} \\ &- J_{1,t}]\aleph^{1,2}_t[G_t-\bar{\mathcal{F}}_{0,2,t}K_{2,t}-J_{2,t}]^{'} \end{aligned} \quad (20)$$

where the subscripts 1 and 2 represent the subsystems 1 and 2 respectively. Similarly, the filtering error equation for subsystem 1 will be stated as:

$$P^{1,2}_{1,t|t}=[I_{n_1}-K_{1,t}\bar{C}_{1,t}]P^{1,2}_{1,t|t-1}[I_{n_1}-K_{2,t}\bar{C}_{2,t}]^{'}+K_{1,t}\aleph^{1,2}_{v,t}K_{2,t} \quad (21)$$

3) Cross-Covariance of Subsystem 2, $h^H_{2,t}$: The cross-covariance of subsystem 2 considers the computation between the modal transition matrices. It can be expressed as:

$$\begin{aligned} &P^{1,2}_{2,t|t} = \\ &[\bar{\mathcal{F}}_{0,t}(I_{n_2}-K_{2,t}\bar{C}_{1,t})-G_t\aleph^{-1}_{\epsilon,t}\bar{C}_{1,t}]P^{1,2}_{2,t|t}[\bar{\mathcal{F}}_{0,t}(I_{n_2}-K_{2,t}\bar{C}_{2,t}) \\ &-G_t\aleph^{-1}_{\epsilon,t}\bar{C}_{2,t}]^{'}+[(\bar{\Psi}_{0,t}+\bar{\Psi}_{1,t})(I_{n_2}-K_{2,t}\bar{C}_{1,t})-G_t\aleph^{-1}_{\epsilon,t}\bar{C}_{1,t}] \\ &P^{1,2}_{2,t|t}[(\bar{\Psi}_{0,t}+\bar{\Psi}_{1,t})(I_{n_2}-K_{2,t}\bar{C}_{2,t})-G_t\aleph^{-1}_{\epsilon,t}\bar{C}_{2,t}]'+[\bar{\Psi}_{2,t}(I_{n_2} \\ &-K_{2,t}\bar{C}_{1,t})-G_t\aleph^{-1}_{\epsilon,t}\bar{C}_{1,t}]P^{1,2}_{2,t|t}[\bar{\Psi}_{2,t}(I_{n_2}K_{2,t}\bar{C}_{2,t})-G_t\aleph^{-1}_{\epsilon,t} \\ &\bar{C}_{2,t}]^{'}+[G_t,(-\bar{\mathcal{F}}_{0,t},-\bar{\Psi}_{0,t},\bar{\Psi}_{1,t},\bar{\Psi}_{2,t})K_{2,t}-G_t\aleph^{-1}_{\epsilon,t}]\aleph^{1,2}_t[G_t, \\ &(-\bar{\mathcal{F}}_{0,t},-\bar{\Psi}_{0,t},\bar{\Psi}_{1,t},\bar{\Psi}_{2,t})K_t-G_t\aleph^{-1}_{\epsilon,t}]^{'} \end{aligned} \quad (22)$$

where $P^{1,2}_{2,t|t}$ is the filtering error covariance for subsystem 2.

Once the information processing has been made for subsystem 1 and 2, it generates two covariance and gain matrices to represent the system. However, this requires functional equivalence to measure invariance across the subsystems such that $f(h^H_{t+1}|h^H_{1,t+1}, h^H_{2,t+1}) = f(h^H_{t+1}|h^H_{1,t+1}) = f(h^H_{t+1}|h^H_{2,t+1})$.

D. Functional Equivalence of Sub-Observers

If the number of sensors used for data fusion have measurement matrices with equal dimensions, such that $C_{1,t} = C_{2,t} = ... = C_{N,t}$, then the subsystem 1 is functionally equivalent to subsystem 2. This requires some inversion of matrices according to the following formula:

$$\begin{bmatrix} A_1 & A_2 \\ A_3 & A_4 \end{bmatrix}^{-1} = \begin{bmatrix} B_1 & B_2 \\ B_3 & B_4 \end{bmatrix} \quad (23)$$

$$(A+CBC^{'})^{-1}=A^{-1}-A^{-1}C(B^{-1}+C^{'}A^{-1}C)^{-1}C^{'}A^{-1} \quad (24)$$

where A_1, A_2, A_3 and A_4 are variables representing a matrix, $B_1 = (A_1 - A_2A_4^{-1}A_3)^{-1}$, $B_2 = -B_1A_2A_4^{-1}$, $B_3 = -A_4^{-1}A_3B_1$, and $B_4 = A_4^{-1} + A_4^{-1}A_3B_1A_2A_4^{-1}$.

Consider the case when the gain matrices of subsystem 1 and 2 are added, such that:

$$\begin{aligned} K_{1,t}+K_{2,t} =& \omega P^{1,2}_{t|t-1}\bar{C}_t^{1,2^{'}}(\bar{C}_{1,t}P^{1,2}_{1,t|t-1}\bar{C}^{'}_{1,t}+R_t)^{-1}+(1-\omega) \\ & P^{1,2}_{t|t-1}\bar{C}_t^{1,2^{'}}(\bar{C}_{2,t}P^{1,2}_{2,t|t-1}\bar{C}_{2,t'}+R_t)^{-1} \end{aligned} \quad (25)$$

where ω is the weight assigned to compute the covariance matrices, $\Xi^{1,2}_{1,t} = (\bar{C}_{1,t}P^{1,2}_{1,t|t-1}\bar{C}^{'}_{1,t} + R_t)^{-1}$ and $\Xi^{1,2}_{2,t} = (\bar{C}_{2,t}P^{1,2}_{2,t|t-1}\bar{C}^{'}_{2,t} + R_t)^{-1}$.

$$\begin{aligned} &K_{1,t}+K_{2,t} \\ &=\omega P^{1,2}_{t|t-1}\bar{C}_t^{1,2^{'}}\begin{bmatrix} R_{1,t}+\Xi^{1,2}_{1,t} & \Xi^{1,2}_{1,t} \\ \Xi^{1,2}_{1,t} & R_{2,t}+\Xi^{1,2}_{1,t} \end{bmatrix}^{-1}+(1-\omega)P^{1,2}_{t|t-1}\bar{C}_t^{1,2^{'}} \\ &\begin{bmatrix} R_{1,t}+\Xi^{1,2}_{2,t} & \Xi^{1,2}_{2,t} \\ \Xi^{1,2}_{2,t} & R_{2,t}+\Xi^{1,2}_{2,t} \end{bmatrix}^{-1} \\ &=\omega P^{1,2}_{t|t-1}\bar{C}^{'}_{1,t}[\overbrace{(R_{2,t}+\Xi^{1,2}_{1,t})}^{A_4})^{-1}\times\overbrace{R_{2,t}}^{A_3} \\ &\overbrace{\big(R_{1,t}+\Xi^{1,2}_{1,t}-\Xi^{1,2}_{1,t}(R_{2,t}+\Xi^{1,2}_{1,t})\Xi^{1,2}_{1,t}\big)}^{B_1}{}^{-1}\times\overbrace{(R_{2,t}+\Xi^{1,2}_{1,t})}^{A_4}{}^{-1} \\ &-\overbrace{(R_{2,t}+\Xi^{1,2}_{1,t})}^{A_4}{}^{-1}\times\overbrace{R_{2,t}}^{A_3} \\ &\overbrace{\big[R_{1,t}+\Xi^{1,2}_{1,t}-\Xi^{1,2}_{1,t}(R_{2,t}+\Xi^{1,2}_{1,t})^{-1}\Xi^{1,2}_{1,t}\big]}^{B_1}{}^{-1}\times\overbrace{\Xi^{1,2}_{1,t}}^{A_2} \\ &\overbrace{(R_{2,t}+\Xi^{1,2}_{1,t})}^{A_4}{}^{-1}]+(1-\omega)P^{1,2}_{t|t-1}\bar{C}_{2,t}[\overbrace{(R_{2,t}+\Xi^{1,2}_{2,t})}^{A_4}{}^{-1}\times\overbrace{R_{2,t}}^{A_3} \\ &\overbrace{\big[R_{1,t}+\Xi^{1,2}_{1,t}-\Xi^{1,2}_{1,t}(R_{2,t}+\Xi^{1,2}_{1,t})^{-1}\Xi^{1,2}_{1,t}\big]}^{B_1}{}^{-1}\times\overbrace{(R_{2,t}+\Xi^{1,2}_{2,t})}^{A_4}{}^{-1} \end{aligned}$$

$$-\overbrace{(R_{2,t}+\Xi_{2,t}^{1,2})}^{A_4}{}^{-1}\times\overbrace{R_{2,t}}^{A_3}\overbrace{[R_{1,t}+\Xi_{2,t}^{1,2}-\Xi_{1,t}^{1,2}(R_{2,t}+\Xi_{2,t}^{1,2})^{-1}\Xi_{2,t}^{1,2}]}^{B_1}{}^{-1}$$
$$\times\overbrace{\Xi_{2,t}^{1,2}}^{A_2}\overbrace{(R_{2,t}+\Xi_{2,t}^{1,2})}^{A_4}{}^{-1} \quad (26)$$

This can be further simplified as:

$$(R_{2,t}+\Xi_{1,t}^{1,2})^{-1}R_{2,t}\big[R_{1,t}+\Xi_t^{1,2}-\Xi_{1,t}^{1,2}(R_{2,t}+\Xi_{1,t}^{1,2})^{-1}\Xi_{1,t}^{1,2}\big]^{-1}$$
$$=\big[\Xi_{1,t}^{1,2}+R_{1,t}(R_{1,t}+R_{2,t})^{-1}R_{2,t}\big]^{-1}R_{2,t}(R_{1,t}+R_{2,t})^{-1} \quad (27)$$

and,

$$(R_{2,t}+\Xi_{1,t}^{1,2})^{-1}-(R_{2,t}+\Xi_{1,t}^{1,2})^{-1}R_{2,t}\times\big[R_{1,t}+\Xi_{1,t}^{1,2}-\Xi_t^{1,2}\times$$
$$(R_{2,t}+\Xi_{1,t}^{1,2})^{-1}\Xi_{1,t}^{1,2}\big]^{-1}\Xi_{1,t}^{1,2}(R_{2,t}+\Xi_{1,t}^{1,2})^{-1}$$
$$=\big[\Xi_{1,t}^{1,2}+R_{1,t}(R_{1,t}+R_{2,t})^{-1}R_{2,t}\big]^{-1}R_{1,t}(R_{1,t}+R_{2,t})^{-1} \quad (28)$$

Similar can be applied for $\Xi_{2,t}^{1,2}$ from equation (27) and (28). Based on (26)-(28), it is further expressed as:

$$K_{1,t}+K_{2,t}=$$
$$\omega P_{t|t-1}^{1,2}\bar{C}_t'\times\big[\bar{C}_{1,t}P_{1,t}^{1,2'}\bar{C}_{1,t}'+R_{1,t}(R_{1,t}+R_{2,t})^{-1}R_{2,t}\big]^{-1}$$
$$\times\big[R_{2,t}(R_{1,t}+R_{2,t})^{-1}R_{1,t}(R_{1,t}+R_{2,t})^{-1}\big]+(1-\omega)P_{t|t-1}^{1,2}C_t'$$
$$\times\big[\bar{C}_tP_{2,t|t-1}^{1,2}\bar{C}_t'+R_{1,t}(R_{1,t}+R_{2,t})^{-1}R_{2,t}\big]^{-1}\times\big[R_{2,t}(R_{1,t}$$
$$+R_{2,t})^{-1}R_{1,t}(R_{1,t}+R_{2,t})^{-1}\big] \quad (29)$$

The interaction of gains with the observation matrix can be expressed as:

$$(K_{1,t}+K_{2,t})\bar{C}_t=$$
$$\omega P_{t|t-1}^{1,2}\bar{C}_t'\times\big[\bar{C}_tP_{1,t|t-1}^{1,2}\bar{C}_t'+R_{1,t}(R_{1,t}+R_{2,t})^{-1}R_{2,t}\big]^{-1}\bar{C}_t+(1$$
$$-\omega)P_{t|t-1}^{1,2}\bar{C}_t'\times\big[\bar{C}_tP_{t|t-1}^{1,2}\bar{C}_t'+R_{1,t}(R_{1,t}+R_{2,t})^{-1}R_{2,t}\big]^{-1}\bar{C}_t \quad (30)$$

Similar goes to its interaction with observation output:

$$(K_{1,t}+K_{2,t})y_t=$$
$$\omega P_{t|t-1}^{1,2}\bar{C}_t'\times\big[\bar{C}_tP_{1,t|t-1}^{1,2}\bar{C}_t'+R_{1,t}(R_{1,t}+R_{2,t})^{-1}R_{2,t}\big]^{-1}\times\big[R_2$$
$$(R_1+R_2)^{-1}y_{1,t}+R_{1,t}(R_{1,t}+R_{2,t})^{-1}y_{2,t}\big]+(1-\omega)P_{t|t-1}^{1,2}\bar{C}_t'$$
$$\times\big[\bar{C}_t'P_{2,t|t-1}^{1,2}\bar{C}_t'+R_{1,t}(R_{1,t}+R_{2,t})^{-1}R_{2,t}\big]^{-1}\times\big[R_{2,t}(R_{1,t}$$
$$+R_{2,t})^{-1}y_{1,t}+R_{1,t}(R_{1,t}+R_{2,t})^{-1}y_{2,t}\big] \quad (31)$$

This marks the functional equivalence here with gain K_t interaction as center of existence for all the calculations. This will be followed by evolving the sub-observers into a synthesis matrix having covariates.

E. Evolution into Synthesis Matrix

The covariates of sub-observers are evolved into a synthesis matrix which is defined to evolve information from subsystem 1 and 2. Covariance matrix $P_{t|t}^{1,2}$ between estimate of sub-observer 1, $\tilde{h}_{1,t|t}$ and sub-observer 2, $\tilde{h}_{2,t|t}$ is represented as:

$$P_{t|t}^{1,2}=R_t\begin{bmatrix}P_{1,t|t}^{1,2} & P_{t|t}^{1,2}\\ P_{t|t}^{2,1} & P_{2,t|t}^{1,2}\end{bmatrix}R_t' \quad (32)$$

where the correlated matrix $P_{t|t}^{1,2}$ is calculated from (25)-(26) as:

$$P_{t|t}^{1,2}=\frac{K_{1,t}+K_{2,t}}{[\omega\bar{C}_t^{1,2'}\Xi_{1,t}^{1,2^{-1}}+(1-\omega)\bar{C}_t^{1,2'}\Xi_{2,t}^{1,2^{-1}}]} \quad (33)$$

with $P_{t|t}^{1,2}{=}P_{t|t}^{2,1'}$. $\hat{h}_{t|t}^H$ is computed by:

$$\hat{h}_{t|t}^H=R_t[\hat{h}_{1,t|t}',\hat{h}_{2,t|t}']' \quad (34)$$

Using the information for processing and relationships between the sensors, the information fusion architecture is established using the IMM algorithm [33]. IMM is preferred over here on other fusion techniques [34], since it considers state hypothesis of multiple models with changing and time-varying dynamics.

F. Interacting Multiple Model (IMM)-Based Fusion

The IMM-based fusion is processed by fusing information of estimated parameters from each installed sensor. The extracted information from level sensor h_t is merged as:

$$\hat{h}_{t|t}^{\text{IMM}}=\sum_{H=\mathcal{U}}^{\mathcal{Z}}p_{\mathcal{U}\mathcal{V}}(h_t^{\mathcal{U}})\hat{h}_{t|t}^{\mathcal{U}} \quad (35)$$

$$P_{t|t}^{\text{IMM}}=\sum_{H=\mathcal{U}}^{\mathcal{Z}}p_{\mathcal{U}\mathcal{V}}(h_t^{\mathcal{U}})(P_{t|t}^{h_{\mathcal{U}}}+[\hat{h}_{t|t}^{h_{\mathcal{U}}}-\hat{h}_{t|t}][\hat{h}_{t|t}^{h_{\mathcal{U}}}-\hat{h}_{t|t}]') \quad (36)$$

where superscript IMM represents the processed variable after any IMM-based fusion performed, $\mathcal{Z}$ is the total number of possible models for height of water-level, $p_{\mathcal{U}\mathcal{V}}$ is the probability that model will switch from sensor $h_t^{\mathcal{U}}$ to $h_t^{\mathcal{V}}$, given the probability of $h_t^{\mathcal{U}}$ at time-instant t. The output of IMM-fusion will determine the residual generation.

G. Residual Generation

The residual of measurements for the estimated parameter could be generated when 1) for each installed sensor, there exists a Lyapunov function $\mathcal{L}_0$ such that for any norm bounded $h_{1,t},h_{2,t}\in\mathbf{R}^n$, the following inequality holds: $\|f(y_t,h_{1,t})-f(y_t,h_{2,t})\|\leq\mathcal{L}_0\|h_{1,t}-h_{2,t}\|$, and 2) the transfer function matrix is strictly positive real, where $K_{1,t},K_{2,t}\in\mathbf{R}^{n\times r}$, and 3) for a given positive definite matrix $\aleph_t>0\in\mathbf{R}^{n\times n}$ at time instant t, there exists covariance matrices $P_t^{1,2}=P_t^{1,2'}>0\in\mathbf{R}^{n\times n}$ and a scalar covariance error R_t at each sensor, such that:

$$\big(\mathcal{F}_t-K_tC_t\big)'P_t^{1,2}\big(\mathcal{F}_t-K_tC_t\big)=-\aleph_t \quad (37)$$

The residual $e_{\text{res,t}}$ can be defined by:

$$e_{\text{res,t}}{=}(\mathcal{F}_t{-}K_tC_t)(h_t{-}\hat{h}_t){+}\Psi[\xi_tf(y_t,h_t){-}\xi_{f,t}f(y_t,h_t)] \quad (38)$$

where ξ_t, $\xi_{f,t}\in\mathbf{R}$ are parameters that change unexpectedly when a variation occurs due to fault injection. The convergence of the residual is guaranteed by the following theorem *III.1*:

Theorem III.1: The filter is asymptotically convergent when no fault occurs ($\xi_t=\xi_{f,t}$), i.e. $\lim_{t\to\infty}C_t(h_t-\hat{h}_t)=0$.

Proof of Theorem III.1: This is proved in the Appendix. ■

Once the residual generation is made, the next step is to evaluate the residual.

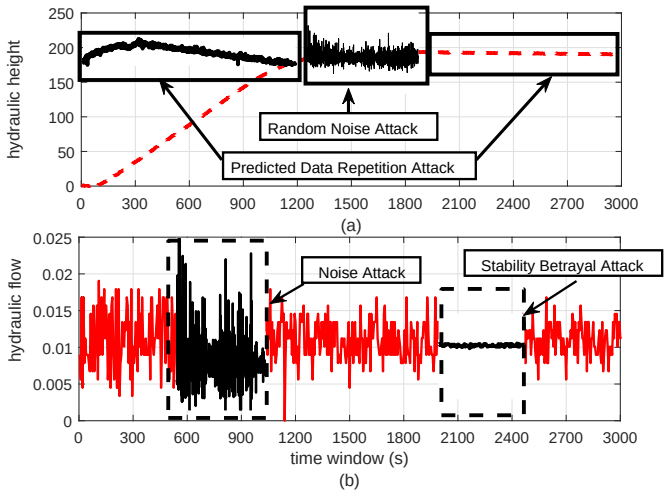

Fig. 3. Fault injections in hydraulic a) height level, and b) flow profile

H. Residual Evaluation using Likelihood Ratio

The residual is based on comparing the likelihood ratio λ. Likelihood ratio is defined here as the ratio of conditional probabilities (under the presence or absence of fault) to a threshold value. It can be represented as:

$$\Gamma_{\text{stat}}(\lambda) = \log(h_{0,t}) - \log(\hat{h}_t) \begin{cases} \leq \eta_{th} \textit{ no fault} \\ > \eta_{th} \textit{ fault} \end{cases} \tag{39}$$

where $\Gamma_{\text{stat}}(\lambda)$ is the test statistic computed using the likelihood ratio λ. η_{th} is a threshold value computed using the innovation principle, which is the difference between the system observed state and its optimal forecast based on information available prior to time t. The threshold value is chosen to ensure a low false alarm probability while making an accurate residual fault evaluation to facilitate the operator.

IV. Evaluation of the Proposed Scheme

The operation of the proposed sub-observer based filter was evaluated on an actual quadruple tank system, the schematic structure of which is already presented in Fig. 2. The system consists of a connected circuit of water tanks, pumps, and actuators which replicate the functionality of a basin in the plant cooling system. The two upper level tanks (tank $\mathcal{W}$ and $\mathcal{X}$) replicate the water from the cool water basin. The bottom level tank $\mathcal{U}$ is supplying water to condenser and steam turbine, whereas tank $\mathcal{V}$ is supplying water to heat recovery steam generator respectively. The piping system is designed such that each pump affects the liquid level of both measured tanks. A portion of the flow from one pump is directed into one of the lower level tanks and the rest is directed to the overhead tank that drains into the other lower level tank. By adjusting the bypass valves of the system, the proportion of the water pumped into different tanks can be adjusted. This alters the interacting relationship between the pump-throughputs and the water level. The pumps were each 12 V due to the large water distribution load.

In this paper, the proposed SOFF scheme is evaluated using the following metrics:

- Attack Detection Time (ADT): Time from the attack occurrence to first sensitive detection of attack.
- Missed Attack Detection Rate (MADR): The ratio of test runs for which the attack occurrence is not detected.
- False Detection Rate (FDR): The ratio of of test runs for which the attack occurrence is detected under no-fault/attack condition.
- Attack Isolation Time (AIT): Time from attack occurrence to first correct isolation of intrusion.
- Missed Isolation Rate (MIR): The ratio of test runs for which the correct attack isolation is not obtained.

In order to evaluate the proposed methodology, a test case has been designed. This test-case has natural system dynamics as well as cyber-attacks, which are spread over the case duration of 3000 seconds. To simulate the attack scenario, several false-data have been injected deliberately and spread over the case duration as follows:

- *First injection*: A random noise attack from 1250–1900 s window on the height sensor.
- *Second injection*: A predicted data-repetition attack initially from 0–1200 s window on the height sensor.
- *Third injection*: A noise attack from 500–1000 s window on the flow sensor.
- *Fourth injection*: A stability betrayal attack from 2000–2500 s window on the flow sensor.

The proposed method here is evaluated against the standard Unscented Kalman filter (UKF) [35], which is a mainstream recursive nonlinear technique. However, UKF is not originally framed to consider cyber-attacks, and that too in an energy-water sector. All estimations are computed using a sampling time, τ_s of 50 milliseconds.

An attacker usually aims to maneuver within the norms defined by the observation model (3) and (12). This would help the attacker's cause of probing and hibernating into the system while not being diagnosed. The first attack is a sparse attack generated from random noise. The attacker wanted to leave an impression to remote monitoring system and the operator that the reference height of water in the basin is reached before time. This was portrayed by having no fluctuation in the height-level achieved. This will further baffle the operations of actuators (pumps and motors). The second attack is a data-repetition attack which can be categorized as a deception attack. Deception attacks usually repeat the past recorded measurements. However, in this case, the attacker had a detailed knowledge about the sea water make-up and the cooled water process. The attacker was able to generate a predicted data-repetition attack at the beginning of the hydraulic profile window. Portraying a full cool water basin, the actuators would stop to function and might also stop the process of pumping water from the sea. This could adversely affect the recirculation process, inlet air-cooling of combustion turbines and steam cycle make-up. The third attack shows the injection of heavy noise in the water-flow profile. This could replicate as if the controller has malfunctioned or there is a blockage in the pipe network or its manifolds. The fourth attack can be categorized as an advanced deception attack. The attacker wanted to show a stationary water as if: 1) there is no supply of sea water to the basin, or 2) there is no demand made from the combined cycle process, which could eventually create a shutdown in the plant. Note the aim of in-

TABLE I

MSE-BASED ESTIMATION COMPARISON ANALYSIS FOR HYDRAULIC HEIGHT SENSOR[1]

Estimate	$\hat{h}_{\text{UKF}}$	$\hat{h}_{\text{SOFF}}$	$\hat{h}_{\text{UKF}}$	$\hat{h}_{\text{SOFF}}$	$\hat{h}_{\text{UKF}}$	$\hat{h}_{\text{SOFF}}$	$\hat{h}_{\text{UKF}}$	$\hat{h}_{\text{SOFF}}$	$\hat{h}_{\text{UKF}}$	$\hat{h}_{\text{SOFF}}$	$\hat{h}_{\text{UKF}}$	$\hat{h}_{\text{SOFF}}$	$\hat{h}_{\text{UKF}}$	$\hat{h}_{\text{SOFF}}$	$\hat{h}_{\text{UKF}}$	$\hat{h}_{\text{SOFF}}$	$\hat{h}_{\text{UKF}}$	$\hat{h}_{\text{SOFF}}$	$\hat{h}_{\text{UKF}}$	$\hat{h}_{\text{SOFF}}$
Time	**0 s–300 s**		**300 s–600 s**		**600 s–900 s**		**900 s–1200 s**		**1200 s–1500 s**		**1500 s–1800 s**		**1800 s–2100 s**		**2100 s–2400 s**		**2400 s–2700 s**		**2700 s–3000 s**	
MSE	0.41	0.0021	0.088	0.0014	0.038	0.0014	0.038	0.0014	0.091	0.0018	0.088	0.0014	0.041	0.0011	0.038	0.0011	0.038	0.0011	0.031	0.0011

[1]In this table, MSE is the mean-square error of estimates, subscript UKF and SOFF are the acronyms of Unscented Kalman filter approach [35] and the proposed SOFF, respectively.

TABLE II

MSE-BASED ESTIMATION COMPARISON ANALYSIS FOR HYDRAULIC FLOW SENSOR

Estimate	$\hat{q}_{\text{UKF}}$	$\hat{q}_{\text{SOFF}}$	$\hat{q}_{\text{UKF}}$	$\hat{q}_{\text{SOFF}}$	$\hat{q}_{\text{UKF}}$	$\hat{q}_{\text{SOFF}}$	$\hat{q}_{\text{UKF}}$	$\hat{q}_{\text{SOFF}}$	$\hat{q}_{\text{UKF}}$	$\hat{q}_{\text{SOFF}}$	$\hat{q}_{\text{UKF}}$	$\hat{q}_{\text{SOFF}}$	$\hat{q}_{\text{UKF}}$	$\hat{q}_{\text{SOFF}}$	$\hat{q}_{\text{UKF}}$	$\hat{q}_{\text{SOFF}}$	$\hat{q}_{\text{UKF}}$	$\hat{q}_{\text{SOFF}}$	$\hat{q}_{\text{UKF}}$	$\hat{q}_{\text{SOFF}}$
Time	**0 s–300 s**		**300 s–600 s**		**600 s–900 s**		**900 s–1200 s**		**1200 s–1500 s**		**1500 s–1800 s**		**1800 s–2100 s**		**2100 s–2400 s**		**2400 s–2700 s**		**2700 s–3000 s**	
MSE	0.064	0.0022	0.088	0.0031	0.089	0.0031	0.066	0.0022	0.064	0.0021	0.064	0.0021	0.069	0.0022	0.081	0.0028	0.069	0.0024	0.064	0.0021

TABLE III

PERFORMANCE EVALUATION OF PROPOSED SOFF SCHEME TOWARDS CYBER-ATTACKS[2]

Metric	**ADT_{UKF}**	**ADT_{SOFF}**	**MADR_{UKF}**	**$\text{MADR}_{\text{SOFF}}$**	**FDR_{UKF}**	**FDR_{SOFF}**	**AIT**	**MIR**
Hydraulic Height Sensor	25.916	16.601	0	0	0.081	0.043	11.831	0.114
Hydraulic Flow Sensor	30.521	19.516	0	0	0.088	0.045	19.324	0.416

[2]In this table, ADT is the attack detection time, MADR is the missed attack detection rate, FDR is the false detection rate, AIT is the attack isolation time and MIR is the missed isolation rate.

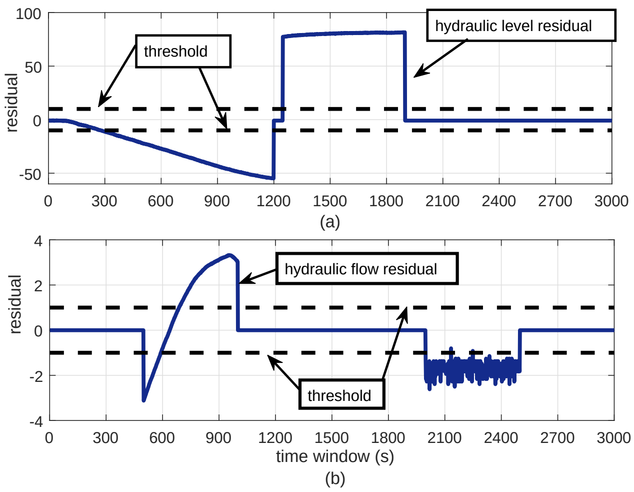

Fig. 4. Residual evaluation in hydraulic a) height-level, and b) flow sensor

jecting a diversified data-injection is to assess the robustness of proposed scheme.

The first and second injections were made on the hydraulic-level sensor as shown in Fig. 3(a). The tracking performance is monitored in all the time windows by comparing both methods in Table I. The first injection considered the system suffering from random noise of few large spikes spread across the 1250–1900 s window. It can be observed that the proposed scheme estimated the output more accurately. This is due to its architecture of approximating information collected from each local sensor, and thereby upgrading each state with the IMM-based feedback. The UKF also performed well due to its non-linear estimation nature. However, its convergence time was demonstrated to be slower than the proposed method. The second injection considered a predicted data-repetition attack from 0–1200 s window on the height sensor. It can be seen that initially UKF was unable to track changes in the parameter. However, around 300 s, it started to converge and track the injection. In contrast, SOFF performed better despite of the fact that attack happened at first instants of hydraulic profile. It was able to track changes in parameter faster and took less time to converge.

The third and fourth injections were made on the hydraulic flow sensor as shown in Fig. 3(b). An MSE-based estimation comparison can be seen in Table II. The third injection was a heavy noise attack in 500–1000 s window. Both methods accurately tracked the change in fluctuations. The amplitude of MSE-error was high for UKF while tracking the profile of flow sensor. This is due to the natural nonlinear instant variations in the hydraulic flow profile, which challenged the capability of unscented transform in UKF for generating the moments. However, the proposed method was more accurate as it did not suffer from deterministic covariance issues. The fourth injection was an attack portraying stationary water from 2000-2500 s window. This was a more challenging scenario since it could diversify the attention of operator and the system towards many components. UKF was unable to track the trap of false stability. This resulted in generating a high MSE value. In contrast, the proposed scheme estimated the variation accurately. The predictive and interactive nature of the algorithm helped to achieve better MSE results.

Once the estimation accuracy is achieved, the likelihood-ratio was deployed to make the residual evaluation. This can be seen in Fig. 4(a)-(b). The threshold selected for the hydraulic level and flow sensor are $\pm$ 10 and $\pm$ 1 respectively. As observed in Fig. 4(a), injected attacks were captured accurately by the thresholds. Similar was the case in Fig. 4(b), where the flow variations were more challenging. The likelihood-ratio based threshold was able to adequately detect all injected variations.

Referring to Table III gives the performance evaluation of the proposed scheme. The metrics ADT (in seconds), MADR, FDR, AIT (in seconds) and MIR are considered for all injected attacks. It can be noted that injected attacks in both height sensor and flow sensor are detected within reasonable time, despite of the fusion of information. The accuracy was also observed for any missed attack detections. Though the isolation ratio is quiet low, there were some missed isolations. SOFF made a better overall performance than the standard UKF. UKF took more

time than SOFF. This could be due to the matrix square root Cholesky transformation computation in a standard UKF.

V. Conclusions

In this paper, the estimation accuracy of an infected water cooling system in a combined cycle power plant has been improved. This is achieved by using an IMM-based fusion approach to consider the instant and time-varying non-linear dynamics. At local-level, the IMM structure is supported by the sub-observer based estimation approach, which further computes the time-delay and cross-covariance between measurements to enhance the observability of the system. As a result, the proposed scheme is able to provide immunity to the system against the injected attacks. One observed limitation of the proposed method is computational complexity, which is increased by information processing at local-level and fusion-level. However, this may be resolved by conducting both computations in parallel using high performance computing (HPC). Future work may lead towards analyzing possible situations in energy-water sector, which may cause vulnerability to the system due to remote monitoring.

Appendix

1) Proof of theorem III.1:

Consider the following Lyapunov function,

$$\mathcal{L}_0\big(e_{\text{res,t}}\big) = e_{\text{res,t}}^{'} P_t^{1,2} e_{\text{res,t}} \tag{40}$$

where $P_t^{1,2}$ is the solution of (37) for residual generation of a given positive definite matrix $\aleph_t$. The corresponding Lyapunov difference for the trajectory $e_{\text{res,t}}$ is:

$$\begin{aligned}
\Delta\mathcal{L}_0 =& \mathbf{E}\big\{\mathcal{L}_0(e_{t+1}|e_t, P_t^{1,2})\big\} - \mathcal{L}_0\big(e_{\text{res,t}}\big) \\
=& \big(\mathcal{F}_{e,t} e_{\text{res,t}} + \Psi_{e,t} V_{e,t}\big)^{'} P_t^{1,2} \big(\mathcal{F}_{e,t} e_{\text{res,t}} + \Psi_{e,t} V_{e,t}\big) \\
& - e_{\text{res,t}}^{'} P_t e_{\text{res,t}} \\
=& e_{\text{res,t}}^{'} \Big[\big(P_t^{1,2}(\mathcal{F}_t - K_t C_t) + (\mathcal{F}_t - K_t C_t)^{'} P_t^{1,2}\big) \\
& + P_t^{1,2} \Psi_t \xi_{f,t} [f(y_t, h_t) - f(y_t, \hat{h}_t)] \Big] e_{\text{res,t}}
\end{aligned} \tag{41}$$

From assumptions and (37), it can be further claimed that:

$$\begin{aligned}
\Delta\mathcal{L}_0 &\leq -e_{\text{res,t}}^{'} \aleph_t e_{\text{res,t}} + 2\|C_t(h_t - \hat{h}_t)\| . |R_t| \xi_{f,t} \mathcal{L}_0 \| e_{\text{res,t}} \| \\
&\leq -\rho \| e_{\text{res,t}} \|^2 < 0
\end{aligned} \tag{42}$$

where ρ is defined to minimize $\aleph_t$, while maintaining its positive definite domain. Thus, $\lim_{t\to\infty} e_{\text{res,t}} = 0$ and $\lim_{t\to\infty} C_t(h_t - \hat{h}_t) = 0$. This completes the proof. ■

References

[1] A. Siddiqui and L. Anadon, "The water energy nexus in Middle East and North Africa," *Energy Policy*, vol. 39, no. 8, pp. 4529–4540, Aug. 2011.

[2] J. S. Maulbetsch, and M. N. Difilippo, "Cost and value of water use at combined-cycle power plants," *PIER Fin. Project Rep.*, CEC-500-2006-034, pp. 1–134, Apr. 2006.

[3] "ABB to automate 225 Megawatt combined cycle power plant In Myanmar," *Ind. News*, Feb. 2017.

[4] "ABB solutions for combined cycle power plants," *Tech. Rep.*, pp. 1–28, Feb. 2011.

[5] "Complete integrated electrical and automation solution for Summit Meghnaghat power plant in Bangladesh," *Tech. Rep.*, pp. 1–2, Jun. 2015.

[6] "Cyber security notification - Meltdown and Spectre, impact on Symphony Plus," *ABB Security Notification Rep.*, ID 8VZZ000522, pp. 1–4, Jan. 2018.

[7] "Conspiracy to commit computer hacking that operates Bowman dam," *https://www.justice.gov/usao-sdny/file/835061/download*.

[8] A. Ostfeld, "Enhancing water-distribution system security through modeling," *J. Water Res. Pla. and Mngmt.*, vol. 132, no. 4, pp. 209–210, Jul. 2006.

[9] C. M. Torres, L. Lavigne, F. Cazaurang, E. A. Garca, D. D. Romero, "Fault detection and isolation on a three tank system using differential flatness," *European Ctrl. Conf.*, pp. 2433-2438, Jul. 2013.

[10] R. Mattone, A. D. Luca, "Nonlinear fault detection and isolation in a three-tank heating system," *IEEE Trans. Ctrl. Sys. Tech.*, vol. 14, no. 6, pp. 1158–1166, 2006.

[11] S. Zhao, B. Huang, and F. Liu, "Detection and diagnosis of multiple faults with uncertain modeling parameters," *J. Water Res. Plan. and Mgmt.*, vol. 25, no. 5, pp. 1873–1881, 2017.

[12] X. He, Z. Wang, Y. Liu, L. Qin, and D. Zhou, "Fault-tolerant control for an internet-based three-tank system: Accommodation to sensor bias faults," *IEEE Trans. Ind. Electronics*, vol. 64, no. 3, pp. 2266–2275, 2017.

[13] D. H. Zhou, X. He, Z. Wang, G. -P. Liu, and Y. D. Ji, "Leakage fault diagnosis for an internet-based three-tank system: An experimental study," *IEEE Trans. Ctrl. Sys. Tech.*, vol. 20, no. 4, pp. 857–870, 2012.

[14] X. He, Z. Wang, L. Qin, and D. Zhou, "Active fault-tolerant control for an internet-based networked three-tank system," *IEEE Trans. Ctrl. Sys. Tech.*, vol. 24, no. 6, pp. 2150–2157, 2016.

[15] M. Jelali, and H. Schwarz, "Nonlinear identification of hydraulic servo-drive systems," *IEEE Ctrl. Sys.*, vol. 15, no. 5, pp. 17–22, 1995.

[16] H. Khan, S. Abou, and N. Sepehri, "Fault detection in electro-hydraulic servo-positioning systems using sequential test of Wald," *Proc. Canadian Conf. Elec. Comp. Engg.*, pp. 1628–1633, 2002.

[17] M. K. Zavarehi, P. D. Lawrence, and F. Sassani, "Nonlinear modeling and validation of solenoid controlled pilot-operated servovalves," *IEEE/ASME Trans. Mechatronics*, vol. 4, no. 3, pp. 324–334, Sep. 1999.

[18] A. S. Musleh, H. M. Khalid, S. M. Muyeen, and A. Al-Durra, "A prediction algorithm to enhance grid resilience towards cyber attacks in WAMCS applications," *IEEE Sys. J.*, vol. 13, no. 1, pp. 710–719, Mar. 2019.

[19] H. M. Khalid, and J. C.-H. Peng, "Immunity towards data-injection attacks using track fusion-based model prediction," *IEEE Trans. Smart Grid*, vol. 8, no. 2, pp. 697–707, 2017.

[20] H. M. Khalid, and J. C.-H. Peng, "A Bayesian algorithm to enhance the resilience of WAMS applications against cyber attacks," *IEEE Trans. Smart Grid, Special Issue Theory of Complex Sys. with Applications to Smart Grid Operations*, vol. 7, no. 4, pp. 2026–2037, 2016.

[21] Z. Skolicki, M. M. Wadda, M. H. Houck, and T. Arciszewski, "Reduction of physical threats to water distribution systems," *J. Water Res. Plan. Mgmt.*, vol. 132, no. 4, pp. 211–217, 2006.

[22] W. Dawsey, B. Minsker, and V. VanBlaricum, "Bayesian belief networks to integrate monitoring evidence of water distribution system contamination," *J. Water Res. Plan. Mgmt.*, vol. 132, no. 4, pp. 234–241, 2006.

[23] M. Propato, "Contamination warning in water networks: General mixed-integer linear models for sensor location design," *J. Water Res. Plan. Mgmt.*, vol. 132, no. 4, pp. 225–233, 2006.

[24] T. M. Baranowski, and E. J. LeBoeuf, "Consequence management optimization for contaminant detection and isolation," *J. Water Res. Plan. Mgmt.*, vol. 132, no. 4, pp. 274–282, 2006.

[25] M. S. Mahmoud, and H. M. Khalid, Book Chapter Title, "Closed loop identification of uncertain systems," *Nova Science Publishers Sig. Processing: New Research*, pp. 135–160, 2013.

[26] R. Doraiswami, L. Cheded, H. M. Khalid, Q. Ahmed, and A. Khoukhi, "Robust control of a closed loop identified system with parametric/model uncertainties and external disturbances," *Intrl. Conf. Sys., Mod. Sim. (ISMS)*, pp. 270–275, January 2010.

[27] P. V. Hof, and R. Schrama, "Identification and control - closed loop issues," *Automatica*, vol. 31, no. 12, pp. 1751–1770, 1995.

[28] K. H. Johansson, and J. L. Nunes, "A multivariable laboratory process with an adjustable zero," *Proceeding of American Control Conference*, pp. 2045–2049, Pennsylvania, USA, June 24-26, 1998.

[29] E. P. Gatzke, and E. S. Meadows, C. Wang, F. J. Doyle III, "Distributed model predictive control of a four-tank system," *J. Comp. Chem. Engg.*, vol. 24, no. 2–7, pp. 1503–1509, 2000.

[30] H. A. Chianeh, J. D. Stigter, and K. J. Keesmana "Optimal input design for parameter estimation in a single and double tank system through direct control of parametric output sensitivities," *J. Process Ctrl.*, vol. 21, no. 1, pp. 111–118, 2011.

[31] S. Skogestad, and I. Postlehwaite, "Multivariable feedback control," *Prentice Hall*, New Jersey, 2001.
[32] S. Shu-Li, M. Jing, "Distributed reduced-order optimal fusion Kalman filters for stochastic singular systems," *Acta Automatica Sinica*, vol. 32, no. 2, pp. 286–290. Mar. 2006.
[33] E. Mazor, A. Averbuch, Y. Bar-Shalom, and J. Dayan, "Interacting multiple model methods in target tracking: A survey," *IEEE Trans. Aerosp. Electron. Syst.*, vol. 34, pp. 103–23, Jan. 1998.
[34] Y. Bar-Shalom and X. Li, "Estimation and tracking: Principles, techniques, and software," *Norwell*, MA: Artech House, 1993.
[35] E. A., Wan, Van der Merwe, R., "The unscented Kalman filter for nonlinear estimation," *Adaptive Sys. Sig. Proc., Comm., Ctrl. Symposium 2000. AS-SPCC. The IEEE 2000*, Lake Louise, Alta, pp. 153–158, Oct. 2000.

Biography

Haris M. Khalid (M'13) received his B.S. (Hons.) degree in Mechatronics and Control Systems Engineering from University of Engineering and Technology (UET), Lahore, Pakistan, in 2007, and the M.S. and Ph.D. degrees in Control Systems Engineering from King Fahd University of Petroleum and Minerals (KFUPM), Dhahran, KSA, in 2009 and 2012, respectively. He is currently an Assistant Professor in Electrical and Electronics Engineering with the Higher Colleges of Technology (HCT), Sharjah Campuses, UAE. In 2012, he joined Distributed Control Research Group (DCRG) at KFUPM, as a Research Fellow. From 2013 to 2016, he worked as a Research Fellow with the Power Systems Research Laboratory (PSRL) at *i*Center for Energy, Masdar Institute (MI), Khalifa University of Science and Technology, Abu Dhabi, UAE, which is an MI-MIT Cooperative Program with Massachusetts Institute of Technology (MIT), Cambridge, MA, USA. During this tenure, he also worked as a Visiting Scholar at Energy Systems, Control & Optimization Lab at ADNOC Research & Innovation Center, Khalifa University of Science and Technology, Abu Dhabi, UAE. He has authored/co-authored over 60 peer-reviewed research publications. He has served as an Energy Specialist in UAE Space Agency (UAESA) 'Tests in Orbit' Competitions, which are partnered with Dream-up and Nano-Racks. He has also served as the Technical Chair of IEEE-ASET'2018-2020 (Seven Group of Conferences) organized in UAE. He is also a reviewer to IEEE Transactions on Power Systems, Neural Network and Learning Systems, Control of Network Systems, Transportation Electrification, and IEEE Systems Journal. His current research interests include power systems, cyber-physical systems, electric vehicles, signal processing, V2G Technology, fault diagnostics, filtering, estimation, and condition monitoring.

S. M. Muyeen (S'03–M'08–SM'12) received his B.Sc. Eng. Degree from Rajshahi University of Engineering and Technology (RUET), Bangladesh formerly known as Rajshahi Institute of Technology, in 2000 and M. Eng. and Ph.D. Degrees from Kitami Institute of Technology, Japan, in 2005 and 2008, respectively, all in Electrical and Electronic Engineering. At the present, he is working as an Associate Professor in the School of Electrical Engineering Computing and Mathematical Sciences, Curtin University, Australia. His research interests are power system stability and control, electrical machine, FACTS, energy storage system (ESS), Renewable Energy, and HVDC system. He has been a Keynote Speaker and an Invited Speaker at many international conferences, workshops, and universities. He has published more than 200 articles in different journals and international conferences. He has published six books as an author or editor. He is serving as Editor/Associate Editor for many prestigious Journals from IEEE, IET, and other publishers including IEEE Transactions of Sustainable Energy, IEEE Power Engineering Letters, IET Renewable Power Generation and IET Generation, Transmission & Distribution, etc. Dr. Muyeen is the senior member of IEEE and Fellow of Engineers Australia.

Jimmy C.-H. Peng (S'04–M'12) received the B.E. and Ph.D. degrees in electrical and computer engineering from the University of Auckland, Auckland, New Zealand, in 2008 and 2012, respectively. He is currently an Assistant Professor in electrical and computer engineering with the National University of Singapore, Singapore. Previously, he was an Assistant Professor with the Masdar Institute (now part of the Khalifa University), Abu Dhabi, United Arab Emirates. In 2013, he was appointed a Visiting Scientist with the Research Laboratory of Electronics, Massachusetts Institute of Technology, Cambridge, MA, USA, where he became a Visiting Assistant Professor in 2014. His research interests include power system stability, cyber security, microgrids, and high-performance computing. He is currently the Secretary of the IEEE Power and Energy Society Working Group on High-Performance Computing for Power Grid Analysis and Operation. He is also a Committee Member for Singapore Standard SS 535.